Volume 19
Number 27
21 July 2023
Pages 5031–5196

# Soft Matter

rsc.li/soft-matter-journal

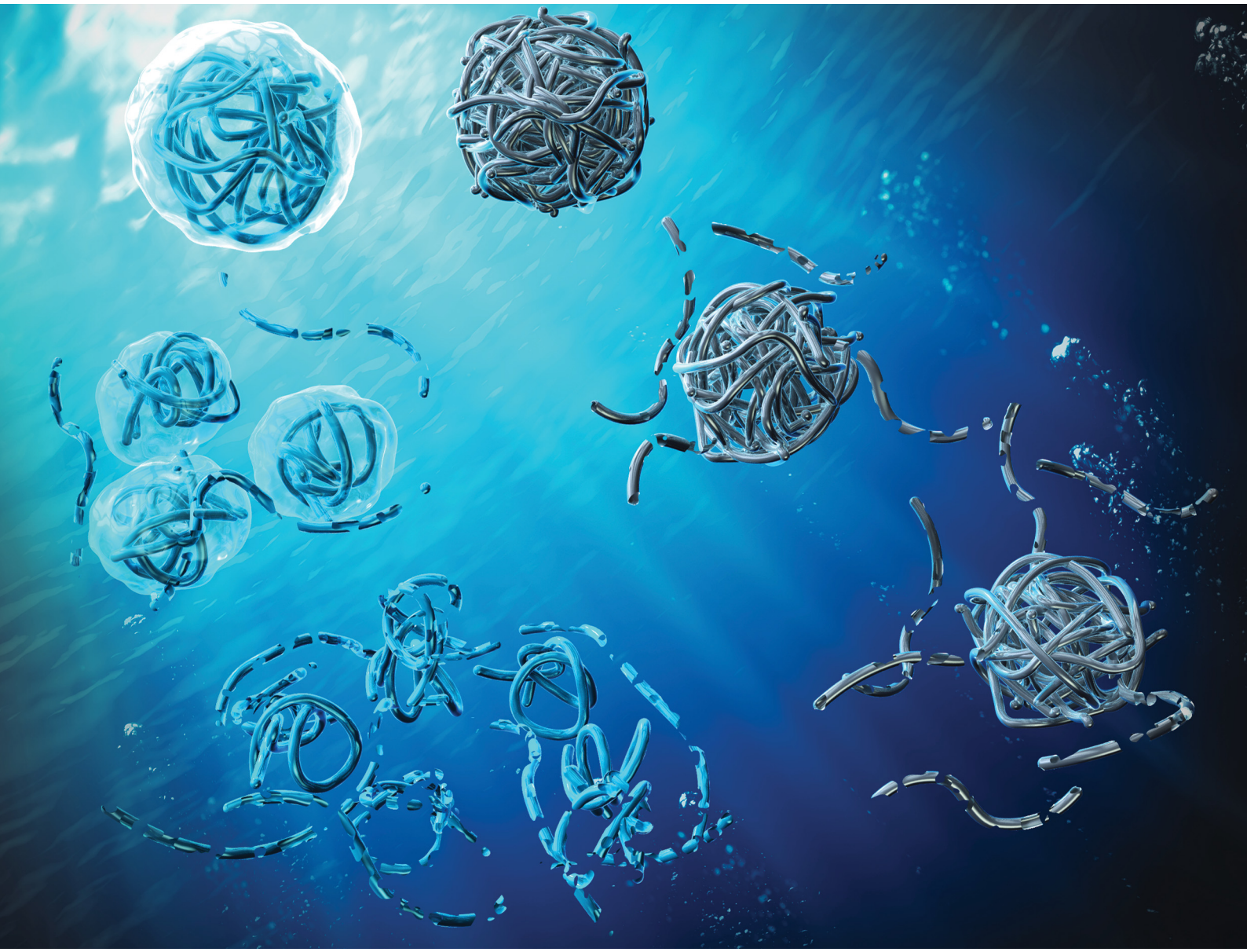

ISSN 1744-6848

ROYAL SOCIETY OF CHEMISTRY

**PAPER**
Takayuki Uchihashi, Daisuke Suzuki *et al.*
Single microgel degradation governed by heterogeneous nanostructures

Soft Matter

PAPER

View Article Online
View Journal | View Issue

Check for updates

Cite this: *Soft Matter*, 2023, **19**, 5068

# Single microgel degradation governed by heterogeneous nanostructures†

Yuichiro Nishizawa, ‡[a] Hiroki Yokoi,‡[a] Takayuki Uchihashi *[cd] and Daisuke Suzuki *[ab]

Received 17th February 2023,
Accepted 26th May 2023

DOI: 10.1039/d3sm00216k

rsc.li/soft-matter-journal

Published on 26 Mays 2023. Downloaded on 16.08.2024 01:04:39.

Although the degradation of colloidal particles is one of the most attractive phenomena in the field of biological and environmental science, the degradation mechanism of single particles remains to be elucidated. In this study, in order to clarify the impact of the structure of a single particle on the oxidative degradation processes, thermoresponsive colloidal particles with chemical cleavage points were synthesized as a model, and their degradation behavior was evaluated using high-speed atomic force microscopy (HS-AFM) as well as conventional scattering techniques. The real-time observation of single-particle degradation revealed that the degradation behavior of microgels is governed by their inhomogeneous nanostructure, which originates from the polymerization method and their hydrophilicity. Our findings can be expected to advance the design of carriers for drug-delivery and the understanding of the formation processes of micro (nano)plastics.

## Introduction

The degradation of colloidal particles is a phenomenon that has been attracting great attention in biological and environmental fields for quite some time. For example, in nature, cells are removed from the body through apoptotic degradation, a process that plays an important role in maintaining health and tissue regeneration.[1] In the field of medical materials, it is expected to be applied to develop carriers for drug-delivery systems (DDS) that transport drug-encapsulated colloids in the blood and release the drug at the site of the disease.[2] For such applications, technologies that are able to selectively degrade the colloidal particles on demand are required. On the other hand, the degradation of colloids is not always beneficial. Recently, concern has arisen that microplastics and nanoplastics produced by the degradation of polymer materials may adversely affect the environment and ecosystems.[3,4] Therefore, a deeper understanding of the degradation of colloidal particles is important for the development of advanced medical technology and the promotion of a more sustainable society.

Against this background, hydrogel microspheres (microgels or nanogels) have been investigated as potential materials for degradable colloids. Microgels are soft colloidal particles with a three-dimensional network composed of hydrophilic or amphiphilic polymers.[5–10] Unlike conventional hard particles such as polystyrene and silica, they are swollen by water, which ensures not only high biocompatibility and colloidal stability, but also allows molecules to diffuse inside the microgels. Moreover, because of the size of the colloid, they can respond to external stimuli such as temperature and pH changes quickly.[5,9] Considering these features, microgels promise high potential as molecular separation materials,[11–14] sensors,[15,16] functional catalysts,[17–19] interface stabilizers,[20–22] and models for colloidal crystals,[23,24] as well as carriers for DDS.[2] In particular, in order to apply microgels as DDS carriers in the body, they must be able to be metabolized after delivering their cargo,[25] and thus, degradable microgels have been developed. For instance, microgels crosslinked by molecules that are cleaved by chemical reactions[26–30] or ultrasonication[31] and microgels characterized by self-crosslinking[32] have been designed. Recently, a synthetic route to microgels has been reported that cross-links the self-assembled polymer chains to reduce the molecular weight of the degradation products.[33–36]

Understanding the degradation behavior of microgels is crucial for designing and controlling their degradability. To date, the degradability of microgels has been evaluated by comparing their morphology before and after degradation using various microscopy techniques[37,38] and by evaluating changes in their relative molecular weight using gel-permeation chromatography (GPC);[27,39] however, these techniques do not allow evaluating real-time changes of the microgel structure. On the other hand,

[a] *Graduate School of Textile Science & Technology, Shinshu University, 3-15-1 Tokida, Ueda, Nagano 386-8567, Japan*
[b] *Research Initiative for Supra-Materials, Interdisciplinary Cluster for Cutting Edge Research, Shinshu University, 3-15-1 Tokida, Ueda, Nagano 386-8567, Japan*
[c] *Department of Physics and Structural Biology Research Center, Graduate School of Science, Nagoya University, Furo-cho, Chikusa-ku, Nagoya, Aichi 464-8602, Japan*
[d] *Exploratory Research Center on Life and Living Systems, National Institutes of Natural Science, 5-1 Higashiyama, Myodaiji, Okazaki, Aichi 444-8787, Japan*

† Electronic supplementary information (ESI) available. See DOI: https://doi.org/10.1039/d3sm00216k

‡ These authors contributed equally to this work.



This journal is © The Royal Society of Chemistry 2023

Published on 26 Mays 2023. Downloaded on 16.08.2024 01:04:39.

using ultraviolet-visible (UV-vis) spectroscopy,[26,40] quartz-crystal microbalancing with dissipation (QCM-D)[41] and dynamic light scattering (DLS)[29] to evaluate the changes in the transmittance of the microgel dispersion, particle weight, and particle size, respectively, allows observing the degradation behavior in real time. However, in these ensemble-based methods, information is averaged and it is not yet clear when and how the degradation proceeds at the single-particle level.

In this context, in order to clarify the relationship between the nanostructure and the degradation behavior of a single microgel, we prepared thermoresponsive microgels with chemical cleavage points as a model and evaluated these using not only a conventional scattering technique, but also high-speed atomic force microscopy (HS-AFM), which has a sufficiently high spatio-temporal resolution to allow a real-time analysis.

## Experimental details

### Materials

*N*-Isopropyl methacrylamide (NIPMAm, purity 97%) and *N*,*N*′-(1,2-dihydroxyethylene)bisacrylamide (DHEA, 97%) were purchased from Sigma-Aldrich and used as received. Potassium peroxodisulfate (KPS, 95%) *N*,*N*′-methylenebis(acrylamide) (BIS, 97%), sodium dodecyl sulfate (SDS, 95%) sodium chloride (NaCl, 99.5 + %), and sodium periodate ($NaIO_4$, 99.5 + %) were purchased from FUJIFILM Wako Pure Chemical Corporation (Japan) and used as received. Distilled and ion-exchanged water was used for the microgel synthesis (EYELA, SA-2100E1). In addition, Fluorosurf® (Fluoro Technology, Japan) was used for the hydrophobic treatment of mica substrates.

### Microgel synthesis

Degradable microgels of poly (NIPMAm-*co*-DHEA) were synthesized *via* aqueous free-radical precipitation polymerization, following a literature procedure.[28] For that purpose, NIPMAm (0.5185 g), DHEA (0.0907 g), and distilled water (25 mL) were placed in a three-necked round-bottom flask (30 mL) and heated to 70 °C under stirring (250 rpm). After removing the dissolved oxygen in the monomer solution by sparging with nitrogen gas (30 min), SDS (0.0172 g) solution and KPS (0.0163 g) solution dissolved in 2.5 mL of distilled water were added. After 4 h, the obtained microgel dispersion was cooled to room temperature to terminate the polymerization. The microgel dispersion was purified using two cycles of centrifugation (15 °C, 70 000 *g*, 30 min)/redispersion in pure water and dialysis against pure water for a week.

### Field-emission scanning electron microscopy (FE-SEM)

The morphology and size uniformity of the microgels were evaluated by FE-SEM (Hitachi Ltd, S-5000 and JSM-IT1800SHL). For that purpose, the diluted microgel dispersions (0.001 wt%) were dropped onto a polystyrene substrate (1 μL) and dried at room temperature. Subsequently, the substrate was sputtered with Pt/Pd (15 mA, 6 Pa, 80 s).

### Dynamic light scattering (DLS)

The hydrodynamic diameter ($D_h$) of the synthesized microgels was evaluated by DLS using a Zetasizer nano S (Malvern Instrument Ltd). The concentration of the microgel dispersions was 0.005 wt% and the ionic strength was adjusted to 1 mM using NaCl. The temperature was varied between 20 °C to 70 °C, whereby equilibration was ensured at each temperature by applying a resting period (10 min) prior to the measurements. The measurements were performed 15 times for 30 s each time, and data from three measurements were averaged. All $D_h$ values were calculated using the Stokes–Einstein equation (Zetasizer software v6.12).

The degradation behavior of the microgels was evaluated from the changes in their hydrodynamic diameter ($D_h$) calculated from the DLS measurements at different temperatures (25 °C to 40 °C). The concentrations of the microgel dispersions and $NaIO_4$ were 0.005 wt% and 50 mM, respectively.

### HS-AFM observation

Using a laboratory-built HS-AFM system with a temperature controller,[42,43] we visualized the nanostructures in aqueous solution during degradation at different temperatures. The HS-AFM images in this study were obtained using an AC10-DS cantilever (length: 10 μm; width: 2 μm; thickness: 90 nm; spring constant: ~0.1 N $m^{-1}$; Olympus, Japan) in tapping mode near the resonance frequency (~600 kHz). The cantilever oscillation was detected using an optical-beam-deflection detector and a red laser ($\lambda_{em}$ = 680 nm). The free oscillation amplitude of the cantilever was set to 5–30 nm. A lock-in amplifier (HF2LI: Zurich Instrument, Switzerland) was used to detect the phase shift of the oscillating cantilever with respect to the driving signal. The experimental procedure was as follows: Fluorosurf® was applied thinly onto the cleaved mica substrate and allowed to air dry for hydrophobic treatment. Then, 3 μL of the microgel dispersion (0.05 wt%) was dropped onto the substrate, and after 5 minutes, the mica surface was washed with pure water to remove the excess microgels. The cantilever holder was filled with water (70 μL). After imaging the structure of the microgels, 10 μL of 400 mM $NaIO_4$ was added to adjust the total concentration to 62.5 mM, and the microgels were degraded in the temperature range from 25 °C to 40 °C.

## Results and discussion

Initially, degradable microgels were synthesized *via* aqueous free-radical precipitation polymerization, which allows the preparation of uniformly sized microgels. In this study, thermoresponsive poly (*N*-isopropyl methacrylamide) (pNIPMAm)-based microgels cross-linked with DHEA, which is cleaved by an oxidation reaction, were synthesized in order to discuss the degradation behavior without self-cross-linking.[28] As a control, pNIPMAm microgels crosslinked with the uncleavable cross-linker BIS were prepared *via* precipitation polymerization. These microgels are denoted as ND10 and NB10, respectively. Here, N, D, B and the number shows NIPMAm, DHEA, BIS and molar

Published on 26 Mays 2023. Downloaded on 16.08.2024 01:04:39.

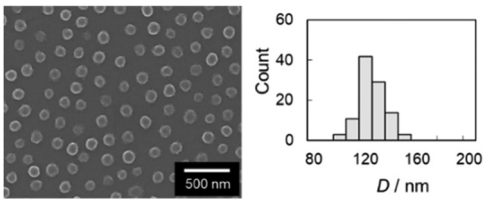


Fig. 1 FE-SEM image and the corresponding size histogram ($N$ = 102) of the ND10 microgels.

ratio of the crosslinker, respectively. The size uniformity of the obtained microgels were confirmed using SEM (ND: 120 ± 10 nm, NB: 159 ± 10 nm) (Fig. 1 and Fig. S1 in the ESI†).

Next, the thermoresponsiveness of the obtained microgels were evaluated *via* DLS measurements. The hydrodynamic diameters of both microgels decreased with increasing temperature, and the volume-transition temperature (VPT), which is defined as the temperature at which the volume change is largest, of ND and NB were determined to be 47 °C and 44 °C, respectively (Fig. 2 and Fig. S2 in the ESI†). The swelling ratio ($\alpha$ = ($D_h$ at 25 °C)$^3$/($D_h$ at 70 °C)$^3$ of ND ($\alpha$ = 6.6) is higher than that of NB ($\alpha$ = 3.6). The higher VPT and $\alpha$ of the ND microgels suggest that DHEA is more hydrophilic than BIS.[44] It should be also noted here that there was no hysteresis in the thermoresponsiveness of either microgel, and that the ND microgels did not degrade during the temperature-change tests. In the presence of 50 mM NaCl, which represents an ionic strength equivalent to that of the oxidant ($NaIO_4$) used for the later degradation tests, the microgels aggregated at 42 °C due to surface deswelling and the effect of electrostatic shielding;[45] thus, we chose the temperature range of 25–40 °C for the degradation tests in this study. The thermoresponsiveness of a single ND microgel was also confirmed *via* HS-AFM (Fig. 3). In this case, the volume decreased significantly from 25 °C (0.99 × $10^{-4}$ μm$^3$) to 32 °C (0.63 × $10^{-4}$ μm$^3$), before it gradually decreased further (0.50 × $10^{-4}$ μm$^3$ at 48 °C). The difference between the thermoresponsiveness in the dispersed states and adsorbed states might be caused by the deformation of microgels on the substrate[46] and hydrophobic interaction between

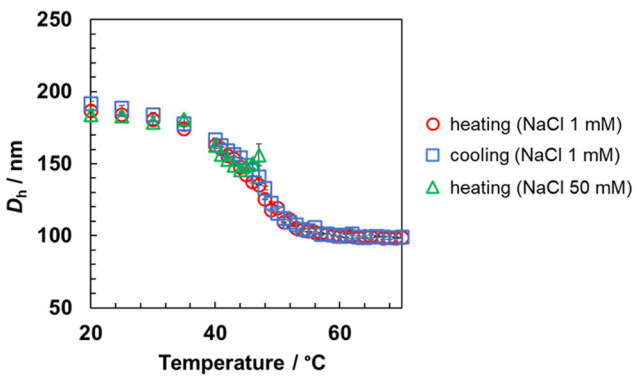


Fig. 2 Temperature dependence of the hydrodynamic diameter ($D_h$) of the ND10 microgels in the presence of different salt concentrations, as derived from the DLS measurements.

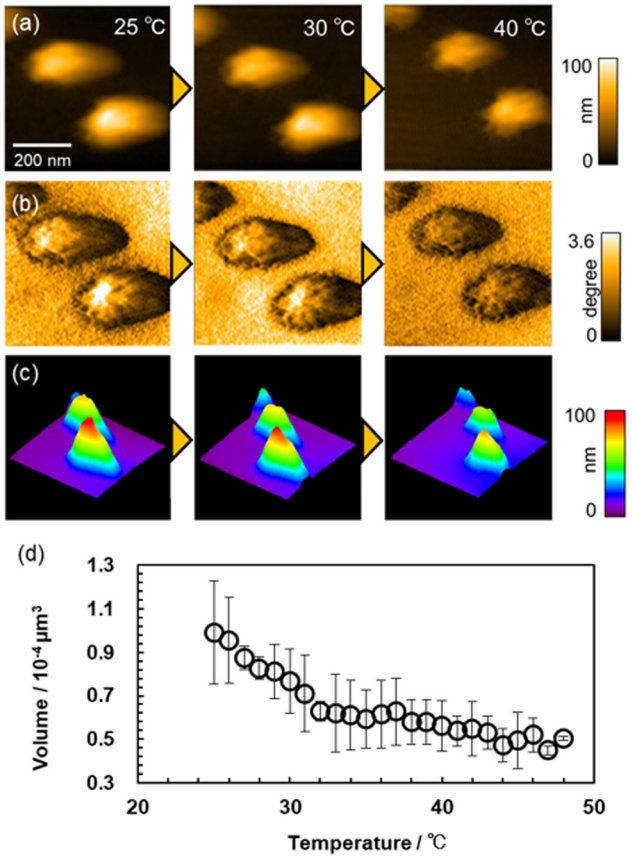


Fig. 3 Temperature dependence of the (a) height images, (b) phase images, (c) 3D images reconstructed from (a and d) the volume ($N$ = 2) of the ND10 microgels in pure water obtained from HS-AFM.

the polymer and hydrophobic surface.[47] Subsequently, the degradation behavior of the ND microgels in the dispersed state at different temperatures was evaluated *via* DLS measurements. At 25 °C, the $D_h$ increased gradually after the addition of the oxidant ($NaIO_4$), before it gradually decreased (Fig. S3a, ESI†) as reported in a previous study.[28] Similar trends were observed at 30 °C (Fig. S3b, ESI†) and 35 °C (Fig. S3c, ESI†). In contrast, at 40 °C, which was defined as the semi-swollen state, little swelling of the microgels was observed, and the decrease in $D_h$ was suppressed (Fig. S3d, ESI†). To clarify the differences in the degradation behavior of the microgels in both the swollen and semi-swollen states, HS-AFM observations were conducted. HS-AFM allows for the addition of solution during imaging;[13,48] therefore, $NaIO_4$ was added during imaging of the microgels adsorbed to hydrophobized mica at 25–40 °C, and the degradation behavior of a single microgel was visualized. As shown in the height image and the phase-contrast image, which reflect the changes in the physical properties of the microgels, we succeeded in visualizing the real-time degradation of ND microgels within the scanning range over 4000 s (Fig. 4 and Movie S1, ESI†). In order to evaluate the degradation behavior in more detail, a single ND microgel was examined; the volume of the microgel gradually decreased in a step-wise fashion, indicating that the degradation of the single microgel

 This journal is © The Royal Society of Chemistry 2023

Published on 26 Mays 2023. Downloaded on 16.08.2024 01:04:39.

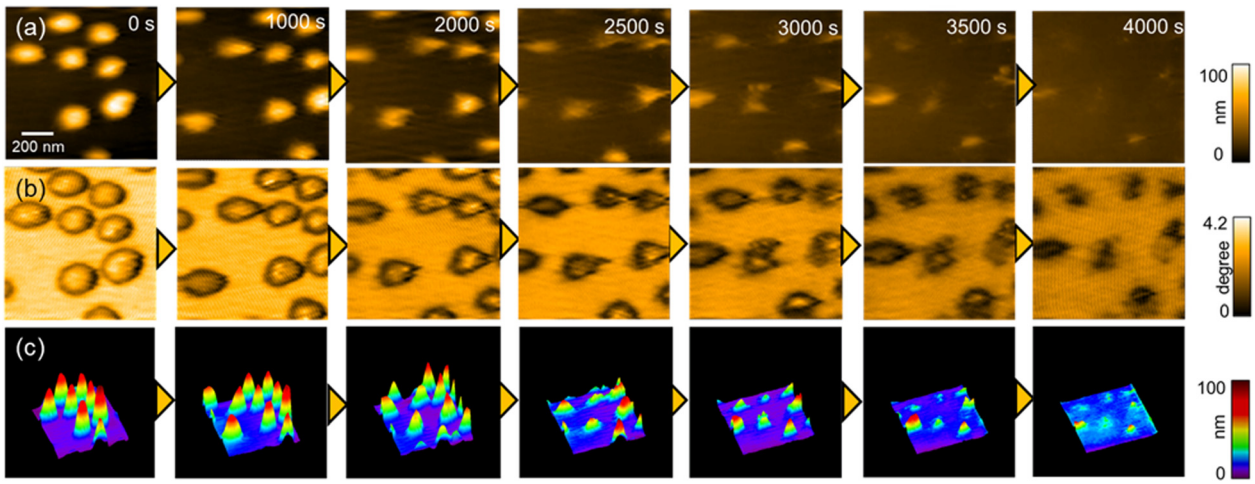


Fig. 4 Time dependence of (a) height images, (b) phase images, and (c) 3D images at 30 °C during the degradation of ND10. The concentration of $NaIO_4$ was 62.5 mM.

is heterogeneous (Fig. 5a, c, d and Movie S2, ESI†). After 2000 s, spherical degradation products with a height of ~20 nm appeared (Fig. 5a, b, c and e). A more detailed observation of the spherical domain structure revealed that each domain degrades over time on different timescales (Fig. 6). It should also be noted here that no significant volume change was observed when the ND microgels were examined in the absence of $NaIO_4$ (Fig. S4, ESI†) or when non-degradable NB microgels were examined in the presence of $NaIO_4$ (Fig. S5, ESI†), indicating that the effect of imaging on the degradation is small.

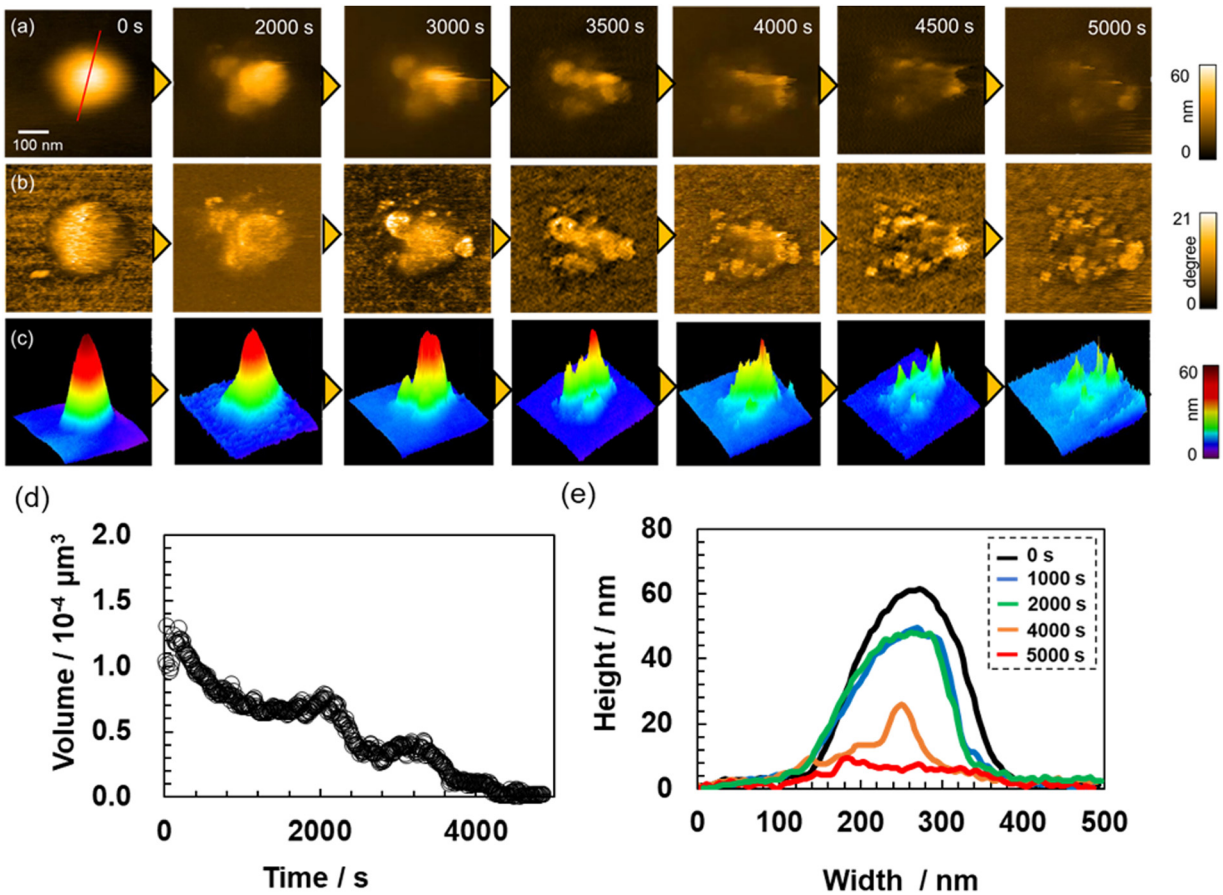


Fig. 5 Time dependence of (a) height images, (b) phase images, (c) 3D images, (d) volume, and (e) cross-sectional profiles corresponding to the red line in (a) during the degradation of ND at 30 °C in the presence of 62.5 mM $NaIO_4$.

Published on 26 Mays 2023. Downloaded on 16.08.2024 01:04:39.

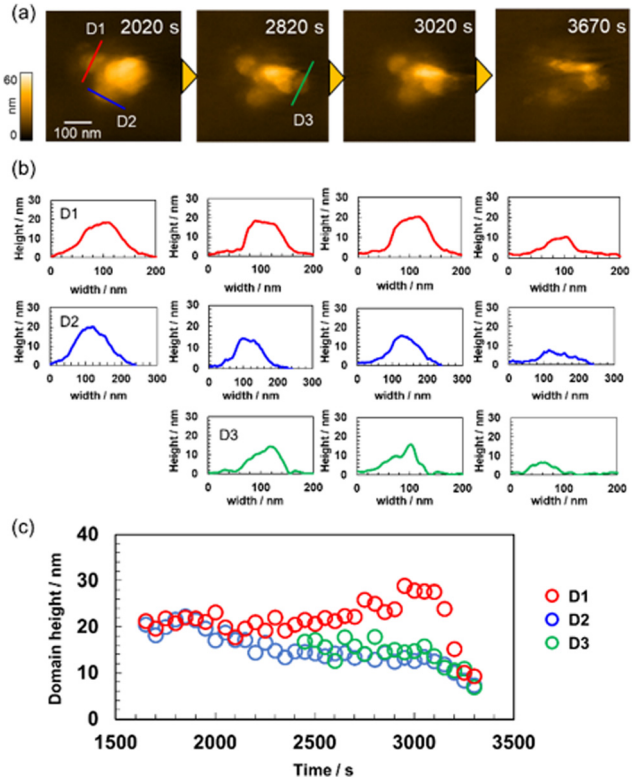


Fig. 6 HS-AFM analysis of the degradation behavior of the spherical degradation products at 30 °C in the presence of 62.5 mM $NaIO_4$: (a) height images, (b) cross-sectional profiles corresponding to each line in (a and c) changes in the domain size during degradation.

A similar trend was observed at 25–35 °C (Fig. S6–8 and Movies S3, S4, ESI†) and microgels with different cross-linking density (Fig. S9, ESI†). Previously, Smith *et al.* have evaluated the degradation behavior of microgels cross-linked with DHEA in the dispersed state using multiangle light scattering, assuming a uniform crosslink density distribution.[28] This method revealed that the particle size increases slightly early during the degradation, before it subsequently decreases. Moreover, the molecular weight decayed sharply, indicating that the degradation process of microgels proceeds as follows: cross-linker degradation causes a decrease in network connectivity, allowing the network to swell, and the microgels then break down into slightly smaller spheres, and finally into linear chains. The same authors also demonstrated that the poly(*N*-isopropyl acrylamide)-based degradable microgels feature a highly cross-linked core and a loosely cross-linked shell structure, whereby the shell layer degrades faster than the core. Additionally, this study clarified that the degradation process of the microgels includes not only the swelling detected by the DLS measurements, but also the formation of the spherical degradation products observed by HS-AFM. Taking into account the discussion above, we assume at this point that the cross-linking density distribution inside the microgels is heterogeneous, and that the degradation products are formed due to the delayed degradation of the highly crosslinked parts. Indeed, it has previously been clarified that spherical heterogeneous nanostructures tens of nanometers in diameter are formed inside microgels during the initial stages of the precipitation polymerization due to the difference in the reactivity ratios between the monomer and crosslinker and the multi-step aggregation process.[49,50]

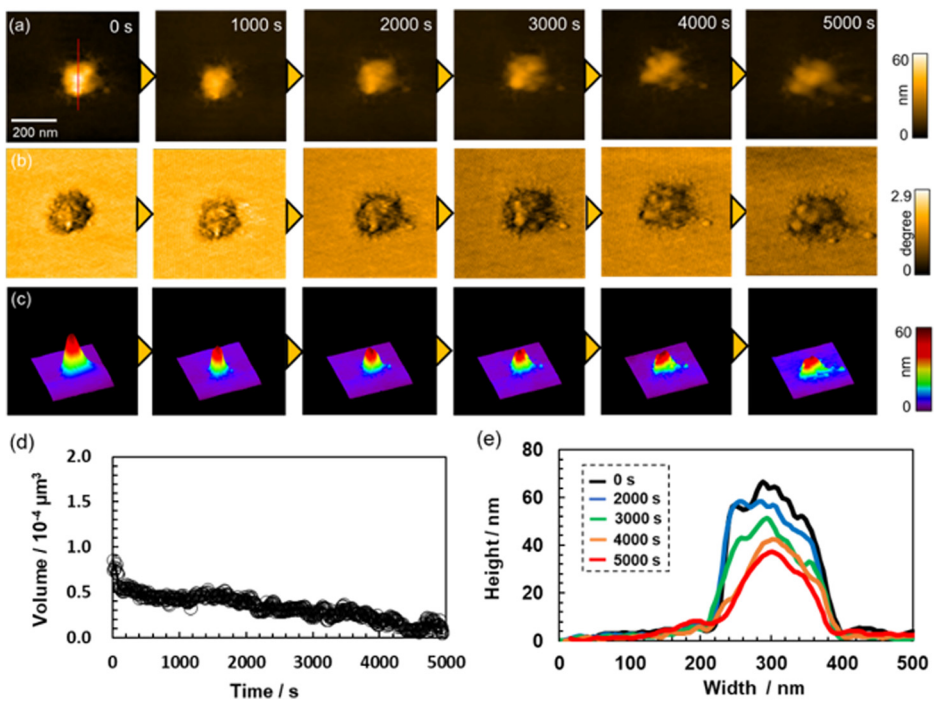


Fig. 7 Time dependence of (a) height images, (b) phase images, (c) 3D images, (d) volume and (e) cross-sectional profiles corresponding to the red line in (a) during the degradation of ND10 at 40 °C. The $NaIO_4$ concentration was 62.5 mM.

 This journal is © The Royal Society of Chemistry 2023

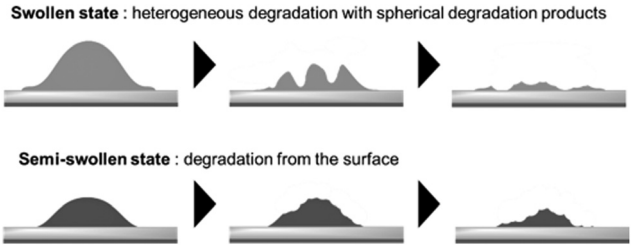


Scheme 1 Schematic illustration of the degradation process with different states.

In contrast, at 40 °C in the semi-swollen state, degradation behavior different from that in the swollen state was observed. A heterogeneous spherical domain nanostructure derived from the precipitation polymerization was visualized inside the ND microgel even before the addition of $NaIO_4$, and the surface of the microgel gradually degraded (Fig. 7 and Fig. S10, Movie S5, ESI†). Wu *et al.* have investigated the catalytic activity of thermoresponsive yolk–shell microgels with an Au nanoparticle core at different temperatures and reported that the reaction rate of hydrophilic substrate was delayed when the microgels were deswollen due to the solvation barriers of the networks, while that of hydrophobic substrate increased.[51] Thus, our results suggested that the diffusion of hydrophilic $NaIO_4$ into the interior of the microparticles was suppressed by the dehydrated polymer chains that constitute the microgels, which change the behavior to degradation from the surface. The different degradation behavior in the swollen and semi-swollen state revealed by HS-AFM observations are conceptually illustrated in Scheme 1.

## Conclusions

In this study, using thermoresponsive, degradable microgels as a model, the relationship between the nanostructure and degradation behavior of a single microgel was investigated *via* high-speed atomic force microscopy (HS-AFM) and light scattering methods. The direct real-time visualization of the degradation behavior *via* HS-AFM revealed that the degradation of microgels in the swollen state not only involves the previously observed swelling process, but also includes the generation of spherical degradation products that originate from the heterogeneous cross-linking-density distribution. In addition, through the evaluation of the temperature dependence of the degradation behavior, we clarified that deswelling of the polymer networks in the microgels causes degradation by hydrophilic oxidants from the surface of the particles. These new insights should be useful for promoting the controlled release of drugs in applications such as drug-delivery systems, as well as for the elucidation of the formation processes of polyethylene and polypropylene micro(nano)plastics, which have recently become a topic of increased interest.

## Author contributions

Y. N. and D. S. wrote the draft of the manuscript. H. Y. characterized the microgels and conducted the HS-AFM the observation of their degradation behaviors. Y. N. and T. U. contributed to experiments and discussion related to the HS-AFM observation. D. S. designed and supervised the overall study.

## Conflicts of interest

There are no conflicts to declare.

## Acknowledgements

D. S. acknowledges a CREST Grant-in Aid (JPMJCR21L2) from the Japan Science and Technology Agency (JST) and a Grant-in-Aid for Scientific Research on Innovative Areas (21H00392) from the Japanese Ministry of Education, Culture, Sports, Science, and Technology (MEXT). T. U. acknowledges a Grant-in-Aid for Scientific Research on Innovative Areas (21H00393) from MEXT.

## Notes and references

1 Y. Wang, H. M. Khan, C. Zhou, X. Liao, P. Tang, P. Song, X. Gui, H. Li, Z. Chen, S. Lui, Y. Cen, Z. Zhang and Z. Li, Apoptotic cell-derived micro/nanosized extracellular vesicles in tissue regeneration, *Nanotechnol. Rev.*, 2022, **11**, 957.
2 J. C. Cuggino, E. R. Osorio Blanco, L. M. Gugliotta, C. I. Alvarez Igarzabal and M. Calderón, Crossing biological barriers with nanogels to improve drug delivery performance, *J. Controlled Release*, 2019, **307**, 221.
3 C. M. Rochman, Microplastics research–from sink to source, *Science*, 2018, **360**, 28.
4 L. Wang, W.-M. Wu, N. S. Bolan, D. C. W. Tsang, Y. Li, M. Qin and D. Hou, Environmental fate, toxicity and risk management strategies of nanoplastics in the environment: Current status and future perspectives, *J. Hazard. Mater.*, 2021, **401**, 123415.
5 R. Pelton, Temperature-Sensitive Aqueous Microgels, *Adv. Colloid Interface Sci.*, 2000, **85**, 1.
6 S. Nayak and L. A. Lyon, Soft Nanotechnology with Soft Nanoparticles, *Angew. Chem., Int. Ed.*, 2005, **44**, 7686.
7 S. Saxena, C. E. Hansen and L. A. Lyon, Microgel Mechanics in Biomaterial Design, *Acc. Chem. Res.*, 2014, **47**, 2426.
8 D. Suzuki, K. Horigome, T. Kureha, S. Matsui and T. Watanabe, Polymeric Hydrogel Microspheres: Design, Synthesis, Characterization, Assembly and Applications, *Polymer J.*, 2017, **49**, 695.
9 M. Karg, A. Pich, T. Hellweg, T. Hoare, L. A. Lyon, J. J. Crassous, D. Suzuki, R. A. Gumerov, S. Schneider, I. I. Potemkin and W. Richtering, Nanogels and Microgels: From Model Colloids to Applications, Recent Developments, and Future Trends, *Langmuir*, 2019, **35**, 6231.
10 Y. Nishizawa, K. Honda and D. Suzuki, Recent Development in the Visualization of Microgels, *Chem. Lett.*, 2021, **50**, 1226.
11 T. Kureha, Y. Nishizawa and D. Suzuki, Controlled Separation and Release of Organoiodine Compounds Using Poly(2-methoxyethyl acrylate)-Analogue Microspheres, *ACS Omega*, 2017, **2**, 7686.

Published on 26 Mays 2023. Downloaded on 16.08.2024 01:04:39.

Published on 26 Mays 2023. Downloaded on 16.08.2024 01:04:39.

12 T. Kureha and D. Suzuki, Nanocomposite Microgels for the Selective Separation of Halogen Compounds from Aqueous Solution, *Langmuir*, 2018, **34**, 837.
13 S. Matsui, K. Hosho, H. Minato, T. Uchihashi and D. Suzuki, Protein Uptake into Individual Hydrogel Microspheres Visualized by High-Speed Atomic Force Microscopy, *Chem. Commun.*, 2019, **55**, 10064.
14 Y. Hoshino, T. Gyobu, K. Imamura, A. Hamasaki, R. Honda, R. Horii, C. Yamashita, Y. Terayama, T. Watanabe, S. Aki, Y. Liu, J. Matsuda, Y. Miura and I. Taniguchi, Assembly of Defect-Free Microgel Nanomembranes for $CO_2$ Separation, *ACS Appl. Mater. Interfaces*, 2021, **13**, 30030.
15 J. H. Holtz and S. A. Asher, Polymerized colloidal crystal hydrogel films as intelligent chemical sensing materials, *Nature*, 1997, **389**, 829.
16 M. Wei, Y. Gao, X. Li and M. J. Serpe, Stimuli-Responsive Polymers and Their Applications, *Polym. Chem.*, 2017, **8**, 127.
17 Y. Lu and M. Ballauff, Thermosensitive Core–Shell Microgels: From Colloidal Model Systems to Nanoreactors, *Prog. Polym. Sci.*, 2011, **36**, 767.
18 T. Kureha, Y. Nagase and D. Suzuki, High Reusability of Catalytically Active Gold Nanoparticles Immobilized in Core–Shell Hydrogel Microspheres, *ACS Omega*, 2018, **3**, 6158.
19 D. Kleinschmidt, M. S. Fernandes, M. Mork, A. A. Meyer, J. Krischel, M. V. Anakhov, R. A. Gumerov, I. I. Potemkin, M. Rueping and A. Pich, Enhanced catalyst performance through compartmentalization exemplified by colloidal L-proline modified microgel catalysts, *J. Colloid Interface Sci.*, 2020, **559**, 76.
20 T. Ngai, S. H. Behrens and H. Auweter, Novel Emulsions Stabilized by pH and Temperature Sensitive Microgels, *Chem. Commun.*, 2005, 331.
21 T. Watanabe, M. Takizawa, H. Jiang, T. Ngai and D. Suzuki, Hydrophobized Nanocomposite Hydrogel Microspheres as Particulate Stabilizers for Water-in-Oil Emulsions, *Chem. Commun.*, 2019, **55**, 5990.
22 Y. Nishizawa, T. Watanabe, T. Noguchi, M. Takizawa, C. Song, K. Murata, H. Minato and D. Suzuki, Durable gelfoams stabilized by compressible nanocomposite microgels, *Chem. Commun.*, 2022, **58**, 12927.
23 T. Okubo, D. Suzuki, T. Yamagata, K. Horigome, K. Shibata and A. Tsuchida, Colloidal crystallization of thermosensitive gel spheres of poly(*N*-isopropylacrylamide) with low degree of cross-linking, *Colloid Polym. Sci.*, 2011, **289**, 1273.
24 D. Suzuki, T. Yamagata, K. Horigome, K. Shibata, A. Tsuchida and T. Okubo, Colloidal crystallization of thermo-sensitive gel spheres of poly (*N*-isopropyl acrylamide). Influence of gel size, *Colloid Polym. Sci.*, 2012, **290**, 107.
25 G. A. Husseini and W. G. Pitt, Micelles and nanoparticles for ultrasonic drug and gene delivery, *Adv. Drug Deliv. Rev.*, 2008, **60**, 1137.
26 S. Nayak, D. Gan, M. J. Serpe and L. A. Lyon, Hollow thermoresponsive microgels, *Small*, 2005, **1**, 416.
27 J. K. Oh, C. Tang, H. Gao, N. V. Tsarevsky and K. Matyjaszewski, Inverse Miniemulsion ATRP: A New Method for Synthesis and Functionalization of Well-Defined Water-Soluble/Cross-Linked Polymeric Particles, *J. Am. Chem. Soc.*, 2006, **128**, 5578.
28 M. H. Smith, E. S. Herman and L. A. Lyon, Network deconstruction reveals network structure in responsive microgels, *J. Phys. Chem. B*, 2011, **115**, 3761.
29 Y. Wang, J. Nie, B. Chang, Y. Sun and W. Yang, Poly-(vinylcaprolactam)-Based Biodegradable Multiresponsive Microgels for Drug Delivery, *Biomacromolecules*, 2013, **14**, 3034.
30 G. Agrawal, R. Agrawal and A. Pich, Dual Responsive Poly(*N*-vinylcaprolactam) Based Degradable Microgels for Drug Delivery, *Part. Part. Syst. Charact.*, 2017, **34**, 1700132.
31 T. Kharandiuk, K. H. Tan, W. Xu, F. Weitenhagen, S. Braun, R. Göstl and A. Pich, Mechanoresponsive diselenide-crosslinked microgels with programmed ultrasound-triggered degradation and radical scavenging ability for protein protection, *Chem. Sci.*, 2022, **13**, 11304.
32 A. C. Brown, S. E. Stabenfeldt, B. Ahn, R. T. Hannan, K. S. Dhada, E. S. Herman, V. Stefanelli, N. Guzzetta, A. Alexeev, W. A. Lam, L. A. Lyon and T. H. Barker, Ultrasoft microgels displaying emergent platelet-like behaviors, *Nat. Mater.*, 2014, **13**, 1108.
33 D. Sivakumaran, E. Mueller and T. Hoare, Temperature-Induced Assembly of Monodisperse, Covalently Cross-Linked, and Degradable Poly(*N*-isopropylacrylamide) Microgels Based on Oligomeric Precursors, *Langmuir*, 2015, **31**, 5767.
34 W. Chen, Y. Hou, Z. Tu, L. Gao and R. Haag, pH-degradable PVA-based nanogels via photo-crosslinking of thermo-preinduced nanoaggregates for controlled drug delivery, *J. Controlled Release*, 2017, **259**, 160.
35 M. J. Simpson, B. Corbett, A. Arezina and T. Hoare, Narrowly Dispersed, Degradable, and Scalable Poly(oligoethylene glycol methacrylate)-Based Nanogels via Thermal Self-Assembly, *Ind. Eng. Chem. Res.*, 2018, **57**, 7495.
36 E. Mueller, S. Himbert, M. J. Simpson, M. Bleuel, M. C. Rheinstadter and T. Hoare, Cationic, Anionic, and Amphoteric Dual pH/Temperature-Responsive Degradable Microgels via Self-Assembly of Functionalized Oligomeric Precursor Polymers, *Macromolecules*, 2021, **54**, 351.
37 X. Zhou, J. Nie, Q. Wang and B. Du, Thermosensitive ionic microgels with pH tunable degradation via in situ quaternization cross-linking, *Macromolecules*, 2015, **48**, 3130.
38 S.-H. Jung, S. Schneider, F. Plamper and A. Pich, Responsive supramolecular microgels with redox-triggered cleavable crosslinks, *Macromolecules*, 2020, **53**, 1043.
39 Y. Wang, J. Nie, B. Chang, Y. Sun and W. Yang, Poly-(Vinylcaprolactam)-Based Biodegradable Multiresponsive Microgels for Drug Delivery, *Biomacromolecules*, 2013, **14**, 3034.
40 S. Nayak and L. A. Lyon, Ligand-Functionalized Core/Shell Microgels with Permselective Shells, *Angew. Chem., Int. Ed.*, 2004, **43**, 6706.
41 J. R. Clegg, A. S. Irani, E. W. Ander, C. M. Ludolph, A. K. Venkataraman, J. X. Zhong and N. A. Peppas, Synthetic networks with tunable responsiveness, biodegradation, and

 This journal is © The Royal Society of Chemistry 2023

Published on 26 Mays 2023. Downloaded on 16.08.2024 01:04:39.

molecular recognition for precision medicine applications, *Sci. Adv.*, 2019, **5**, eaax7946.
42 T. Ando, T. Uchihashi and S. Scheuring, Filming Biomolecular Processes by High-Speed Atomic Force Microscopy, *Chem. Rev.*, 2014, **114**, 3120.
43 S. Matsui, Y. Nishizawa, T. Uchihashi and D. Suzuki, Monitoring Thermoresponsive Morphological Changes in Individual Hydrogel Microspheres, *ACS Omega*, 2018, **3**, 10836.
44 C. M. Nolan, C. D. Reyes, J. D. Debord, A. J. García and L. A. Lyon, Phase Transition Behavior, Protein Adsorption, and Cell Adhesion Resistance of Poly(ethylene glycol) Cross-Linked Microgel Particles, *Biomacromolecules*, 2005, **6**, 2032.
45 Y. Nishizawa, T. Inui, R. Namioka, T. Uchihashi, T. Watanabe and D. Suzuki, Clarification of Surface Deswelling of Thermoresponsive Microgels by Electrophoresis, *Langmuir*, 2022, **38**, 16084.
46 Y. Nishizawa, H. Minato, T. Inui, I. Saito, T. Kureha, M. Shibayama, T. Uchihashi and D. Suzuki, Nanostructure and thermoresponsiveness of poly(*N*-isopropyl methacrylamide)-based hydrogel microspheres prepared via aqueous free radical precipitation polymerization, *RSC Adv.*, 2021, **11**, 13130.
47 X. Shaulli, R. Rivas-Barbosa, M. J. Bergman, C. Zhang, N. Gnan, F. Scheffold and E. Zaccarelli, Probing temperature responsivity of microgels and its interplay with a solid surface by super-resolution microscopy and numerical simulations, *ACS Nano*, 2023, **17**, 2067.
48 S. Matsui, T. Kureha, S. Hiroshige, M. Shibata, T. Uchihashi and D. Suzuki, Fast Adsorption of Soft Hydrogel Microspheres on Solid Surfaces in Aqueous Solution, *Angew. Chem., Int. Ed.*, 2017, **56**, 12146.
49 Y. Nishizawa, S. Matsui, K. Urayama, T. Kureha, M. Shibayama, T. Uchihashi and D. Suzuki, Non-Thermoresponsive Decananosized Domains in Thermoresponsive Hydrogel Microspheres Revealed by Temperature-Controlled High-Speed Atomic Force Microscopy, *Angew. Chem., Int. Ed.*, 2019, **58**, 8809.
50 Y. Nishizawa, H. Minato, T. Inui, T. Uchihashi and D. Suzuki, Nanostructures, Thermoresponsiveness, and Assembly Mechanism of Hydrogel Microspheres during Aqueous Free-Radical Precipitation Polymerization, *Langmuir*, 2021, **37**, 151.
51 S. Wu, J. Dzubiella, J. Kaiser, M. Drechsler, X. Guo, M. Ballauff and Y. Lu, Thermosensitive Au-PNIPA Yolk–Shell Nanoparticles with Tunable Selectivity for Catalysis, *Angew. Chem., Int. Ed.*, 2012, **51**, 2229.